HHS Public Access

Author manuscript

Dev Dyn. Author manuscript; available in PMC 2021 November 03.

Published in final edited form as:

Dev Dyn. 2021 November ; 250(11): 1600–1617. doi:10.1002/dvdy.353.

Drebrin, an actin-binding protein, is required for lens morphogenesis and growth

Shruthi Karnam[1], **Rupalatha Maddala**[1], **Jonathan A Stiber**[2], **Ponugoti V Rao**[1,3,*]

[1.]Department of Ophthalmology, Duke University School of Medicine, Durham, NC. USA

[2.]Department of Medicine, Duke University School of Medicine, Durham, NC. USA

[3.]Department of Pharmacology and Cancer Biology, Duke University School of Medicine, Durham, NC. USA

Abstract

Background: Lens morphogenesis, architecture, and clarity are known to be critically dependent on actin cytoskeleton organization and cell adhesive interactions. There is limited knowledge, however regarding the identity and role of key proteins regulating actin cytoskeletal organization in the lens. This study investigated the role of drebrin, a developmentally regulated actin-binding protein, in mouse lens development by generating and characterizing a conditional knockout (cKO) mouse model using the Cre-LoxP recombination approach.

Results: Drebrin E, a splice variant of *DBN1* is a predominant isoform expressed in the mouse lens and exhibits a maturation-dependent downregulation. Drebrin co-distributes with actin in both epithelium and fibers. Conditional deficiency (both haploinsufficiency and complete absence) of drebrin results in disrupted lens morphogenesis leading to cataract and microphthalmia. The drebrin cKO lens reveals a dramatic decrease in epithelial height and width, E-cadherin, and proliferation, and increased apoptotic cell death and expression of α-smooth muscle actin, together with severely impaired fiber cell organization, polarity, and cell-cell adhesion.

Conclusions: This study demonstrates the requirement of drebrin in lens development and growth, with drebrin deficiency leading to impaired lens morphogenesis and microphthalmia.

Keywords

Cytoskeleton; development; differentiation; epithelium; eye; polarity

[*]Correspondence: P. V. Rao, Ph.D., Duke Eye Center, Durham, NC. USA. 27710, Phone: 919-681-5883, Fax: 919-684-8983, p.rao@duke.edu.

AUTHOR CONTRIBUTIONS

SK: Conceptualization; data curation; formal analysis; methodology; writing-original draft; **RM**: Data curation; formal analysis; methodology; writing-review; editing **JAS**: Methodology; resources; writing-review; editing; **PVR:** Conceptualization; funding acquisition; resources; supervision; writing- review; editing.

DECLARATION OF INTEREST

The authors declare no conflict of interest.

1. INTRODUCTION

The avascular and transparent ocular lens plays a crucial role in vision by focusing light onto the retina. The lens develops from the lens vesicle (LV), which is formed upon invagination of the lens placode ectoderm. Following separation of the LV from the surface ectoderm, posterior cells of the LV elongate and differentiate into lens primary fibers, while the anterior cells form the epithelium covering the anterior surface of the lens. After primary fibers fill the LV, epithelial cells at the equator exit the cell cycle and differentiate into secondary fibers.[1] Both primary and secondary fibers establish apical to apical cell adhesive interactions with epithelial cells at the anterior while at the posterior, they form adhesions with the extracellular matrix of the capsule.[2, 3] Lens fibers undergo terminal differentiation and eventually lose all cellular organelles, including the nuclei, and assume a radial packing organization with perfect hexagonal symmetry.[4, 5] Since development and differentiation of secondary lens fibers continues throughout life, this results in newly formed fibers laying over older fibers. Moreover, since the lens is enclosed by a thick capsule, all cells formed from birth onwards are retained within the organ with no turnover (Fig. 1; A schematic illustration of the lens architecture).[4] Various transcriptional factors and growth factor signaling mechanisms are known to be required for lens specification, morphogenesis, and growth.[1, 6] Developmental defects in the lens affect not only vision but the morphogenesis of many other tissues of the eye as well including tissues of the anterior segment iridocorneal angle and the retina, and commonly associating with microphthalmia. These associations inform our understanding of the influence and importance of normal lens development and growth for the development and function of other tissues of the eye.[1, 6]

The lens cytoskeleton consists of all three types of cytoskeletal networks including microfilaments, microtubules, and intermediate filaments.[5, 7, 8] The role and importance of actin filament organization and dynamics, and actin cytoskeletal organization in lens developmental events has been extensively studied.[5] These events include invagination of the lens placode, separation of lens vesicle from the surface ectoderm, epithelial morphogenesis, polarity, epithelial differentiation and elongation into fiber cells, fiber cell migration, maintenance of fiber cell hexagonal shape, membrane organization, and cell-cell adhesion.[5, 9–17] Further, it is also well recognized that actin cytoskeletal reorganization and assembly are involved in the etiology of secondary cataract, which is driven primarily by the trans differentiation of epithelial cells into mesenchymal cells.[18–20] Despite the recognition that the actin cytoskeleton plays a critical role in lens morphogenesis, growth, and architecture, our knowledge of actin-binding proteins that play a key role in regulating lens actin cytoskeletal organization and dynamics is very limited.[5, 16]

The transcriptome profile of mouse lens based on RNA-seq analysis revealed expression of drebrin.[21, 22] Drebrin is a well-characterized actin-binding protein initially discovered as a developmentally regulated protein expressed in the brain.[23] Drebrin is encoded by a single gene (*DBN1*) that gives rise to two isoforms; Drebrin A (adult) and E (embryonic) via transcript alternative splicing.[23] While drebrin A expression is highly specific to neurons, drebrin E is expressed in various tissues.[23–27] In the brain, isoform conversion from drebrin E to drebrin A occurs in parallel with synaptogenesis.[23] Drebrin-decorated F-actin has been shown to slow actin treadmilling, decrease the rate of actin filament depolymerization,

and play a crucial role in remodeling and regulating mechanical properties of the actin filament.[24, 27–33] Drebrin belongs to an actin-depolymerizing factor homology (ADF-H) domain protein family,[34] containing an actin-binding domain and Homer-binding motifs in addition to the ADF-H domain.[35] Serving as a multifunctional cytoskeletal regulator, drebrin competes against several other proteins for binding to F-actin including tropomyosin, fascin, α-actinin, caldesmon, and cofilin. Drebrin interacts with microtubules and localizes to focal adhesions, adherens junctions, and gap junctions, to regulate many cellular processes.[28, 30, 36–40] Drebrin participates in the regulation of actin dynamics during tumor development, progression, and metastasis, and drebrin dysregulation and deficiency are known to be associated with various neurological diseases.[23, 35, 41–43]

Based on the known role of drebrin in F-actin stability and microtubule interaction, we were interested in exploring the role this protein might play in lens development and growth. To this end, we developed and characterized a drebrin conditional knockout mouse model. Our study demonstrates that drebrin plays an essential role in lens morphogenesis and that the absence of this protein leads to impaired lens development and microphthalmia.

2. RESULTS

2.1. Expression profile and maturation dependent downregulation of drebrin E in the mouse lens

The expression profile of drebrin isoforms E and A in the P2 and P21 mouse lens was initially evaluated by RT-PCR analysis of RNA and compared to that in brain tissue. This analysis revealed that drebrin E is the most abundantly expressed isoform in the neonatal mouse lens (P2), with P21 lenses exhibiting much-reduced levels. Expression levels of drebrin A were minimal in both P2 and P21 lenses, in contrast, drebrin A was the most abundant isoform expressed in both neonatal and adult brain tissue as reported earlier.[23] On the other hand, drebrin E expression was detected only in neonatal brain samples (Fig. 2A). Subsequent immunoblotting analysis of P1 and P30 mouse lens and brain homogenates (800 × g supernatant, 30 μg protein) using a drebrin A specific antibody confirmed the presence of drebrin A only in the brain samples (Fig. 2B). Drebrin E was readily detectable in neonatal lenses, with levels of the protein gradually decreasing from the P1 to P30 stage and being undetectable in P90 lenses (30 μg of 800 × g lens supernatants) as assessed by immunoblotting, indicating a postnatal maturation associated downregulation of drebrin E expression in the mouse lens (Fig. 2C). Hereafter, drebrin E is referred to as drebrin through the rest of this manuscript. Immunoblotting analysis of cytosolic and membrane-enriched fractions from P30 lenses also revealed that drebrin exists as a predominantly cytosolic protein (Fig. 2D), being expressed in both, the lens epithelium (pooled sample from n=4 lenses) and fiber mass (pooled sample from n=two lenses) from P1 mice (Fig. 2E). Additionally, immunofluorescence analysis of E13.5, E16.5, and P1 mouse lens sagittal plane cryosections revealed that drebrin exhibits a relatively prominent localization at the interface of the apical junctions of epithelial and fiber cells (Fig. 2F, arrowheads), and at the fulcrum region (Fig. 2F, arrows). Inserts in Fig. 2F (E16.5 specimen) highlight these distribution characteristics of drebrin. In paraffin-embedded, sagittal sections of P21 lenses drebrin was found to distribute to both, the epithelium and fiber cells (Fig. 2F).

2.2. Drebrin co-distributes with actin, ZO-1, and N-cadherin in the lens

Sagittal and equatorial sections (paraffin-embedded) derived from E17.5, P1, and P30 mouse lenses were analyzed by immunofluorescence in conjunction with confocal imaging to evaluate the cellular distribution pattern and colocalization of drebrin with actin and cell-cell junctional proteins. The results reveal that drebrin presents a distribution pattern very similar to that of β-actin in these lenses. In E17.5 lens sagittal sections, drebrin exhibits co-localization with β-actin at the apical junctions of epithelial and fiber cells with a prominent co-distribution at the fulcrum region (Fig. 3A, arrows). The merged images of drebrin and β-actin staining in lens epithelium reveals their co-distribution at the cell-cell junctions as well (Fig. 3B, arrowhead). Drebrin similarly colocalized with ZO-1 in P1 lenses (Fig. 3C, merged panel). Additionally, drebrin and β-actin were found to exhibit identical distribution patterns in P30 lens fibers, with intense localization at the vertices of the hexagonal fiber cells from equatorial lens sections (Fig. 3D, arrows; images were captured from the lens cortical region, 50 μm from the epithelium). Drebrin was also found to colocalize with N-cadherin at the vertices of hexagonal fiber cells in P30 lens equatorial sections (Fig. 3E).

2.3. Conditional deficiency of drebrin impairs lens morphogenesis leading to microphthalmia and cataract phenotype

To investigate the role of the actin-binding protein, drebrin in lens morphogenesis and architecture, we generated a drebrin (*DBN1*) conditional knockout (cKO) mouse model with the Cre-LoxP recombinant approach using drebrin floxed mice and transgenic mice expressing Cre recombinase in a lens-specific manner (Le-Cre). The generation of drebrin floxed mouse, which is maintained on a C57BL/6J genetic background, has been described previously.[44] The Le-Cre transgenic mouse model has been extensively used in prior research studies.[45] The drebrin cKO mice used in this study were from the seventh or higher generation. Fig. 4A shows representative images confirming conditional deletion of *DBN1* based on tail DNA genotyping. Littermate drebrin floxed mice were used as controls for the cKO mice. Lenses derived from the cKO mice showed a complete absence of drebrin, whereas the drebrin conditional haploinsufficient (cHet) lenses showed much reduced (> 60%) levels of drebrin compared to littermate control lenses. Fig. 4B shows a representative immunoblot of drebrin in littermate control, drebrin cHet, and drebrin cKO mouse lenses. Consistent with the immunoblotting data, immunofluorescence analysis of drebrin in P1 lens cryosections revealed the absence of drebrin in cKO mice and much-reduced staining in the cHet mice relative to that observed in littermate control mice (Fig. 4C). The distribution of drebrin in the retina of cKO and cHet mouse was not affected, confirming that the conditional deficiency of drebrin is specific to the lens in the cKO mouse. Since expression of drebrin was not very prominent in other tissues of the anterior segment of control eyes, we could not compare the levels of drebrin in ciliary, cornea, or iridocorneal angle tissues of the cKO mice with control mice. Fig. 4D shows impaired lens morphogenesis in both drebrin cHet and cKO mice (P1) compared to littermate control mice. Tissue sections stained for F-actin using rhodamine-phalloidin (Fig 4D) revealed dramatic reduction of phalloidin fluorescence in both drebrin cHet and cKO lenses compared to control lenses (Fig. 4E).

One of the overt and consistent bilateral ocular phenotypes found in both cKO and drebrin cHet mice was microphthalmia (reduced eye size) compared to littermate controls (floxed) and age-matched Le-Cre mice. This phenotype was evident even in the neonatal (P1) mice. Eye weight was significantly decreased in both drebrin cHet and cKO neonatal (P1) mice, by ~ 54% and 65%, respectively, compared to littermate control mice (Fig. 4F). Fig. 4G depicts a representative image of microphthalmic eyes derived from P21 cKO mice compared to the respective littermate control mice. Fig. 4H shows the intense nuclear cataract phenotype in both P10 cHet and cKO drebrin mouse lenses. Additionally, we periodically compared the lens and eye phenotype of drebrin cKO with age-matched Le-Cre transgenic mice. The Le-Cre transgenic mice in our study did not show any eye or lens abnormalities compared to control mice. The P2 lens morphology of the Le-Cre mouse (stained for β-actin) shown in Fig. 4I was also found to be normal and comparable to control lenses.

To gain further insight into the effects of drebrin absence on lens morphogenesis, growth, and architecture, we performed histological analysis (paraffin-embedded sagittal sections) of embryonic (E13.5, and E17.5), neonatal (P1), and weanling (P8) drebrin cKO mouse eyes and littermate control eyes using hematoxylin and eosin staining. Starting from E13.5, drebrin cKO mouse lenses exhibit overt abnormalities in lens fiber cell organization and the distribution pattern of nuclei in fiber cells. These abnormalities increased progressively between the E13.5 to P8 stages and are characterized by disorganization and degeneration of lens fibers, together with large gaps and accumulation of vacuoles within the fiber mass of drebrin cKO lenses, relative to the littermate control mouse lenses. Starting at E17.5, in addition to the progressive and dramatic decrease in lens size in the drebrin cKO mice, the lens was found to be fused with the cornea, iris and iridocorneal angle leading to disruption of the development of iridocorneal angle (arrow) compared to the control eyes (Fig. 5A), although the lens capsule appears to be intact. Fig. 5A shows representative images of lens histological changes in the drebrin cKO mouse relative to lenses from corresponding littermate controls of different age groups.

Since both the drebrin conditional haploinsufficient and cKO mice exhibit a severe lens phenotype evident starting from the embryonic stages, this impeded our ability to isolate intact lenses for analysis. Most of the analyses described in this study were therefore based on the immunofluorescence analyses using either embryonic or P1 lens specimens.

We also examined lens epithelial integrity and primary fiber cell elongation in the E11.5 drebrin cKO lens using cryosections stained for E-Cadherin and using rhodamine-phalloidin. As shown in Fig. 5B, at E11.5, there seems to be no obvious difference in the epithelium, and primary fiber cell elongation between drebrin cKO and littermate control lenses. Fulcrum formation was evident in the control lens (arrow) but not in the drebrin cKO lens.

2.4. Impaired actin and spectrin cytoskeletal organization, cell-cell junctions, and epithelial phenotype in drebrin cKO lens

One of the well-recognized activities of drebrin is its interaction with actin to stabilize the actin filament network and cell adhesive interactions.[24, 28, 38, 46] To determine how the absence of drebrin may influence these interactions, paraffin-embedded sagittal sections from P1 lenses of drebrin cKO and littermate control mice were immunostained for β-actin

and β2-spectrin. Staining for both actin and spectrin was markedly reduced in the drebrin cKO lens, being pronounced in drebrin cKO lens fiber cells compared to control lens fibers (Fig. 6A and C). The reduction in actin and spectrin staining of lens fibers is associated with fiber cell disorganization (loss of the typical concave orientation of fiber cells required for lens suture formation at both the anterior and posterior regions) and alteration in lens shape from spherical to conical in drebrin cKO mice compared to control lenses (Fig. 6A and C). Another prominent phenotype observed in the drebrin cKO lenses was a significant decrease in lens epithelial height (≥50% of control; indicated with double-headed arrows in Fig. 6B, D and E) and epithelial sheet length (~40% of control; marked with yellow line drawing in Fig. 6C and F) along with an apparent reduction in the number of nuclei compared to control mouse lenses (Fig. 6B and D).

In addition to assessing actin and spectrin cytoskeletal organization, we evaluated distribution profiles of cell-cell junctional proteins including ZO-1, E-cadherin, and N-cadherin, each of which is known to play a vital role in regulating lens morphogenesis, polarity, and growth.[2, 47–49] As shown in Fig. 7, the distribution pattern of ZO-1 (arrows), E-cadherin, and N-cadherin was markedly disrupted in the drebrin cKO lenses (E17.5, or P1, paraffin-embedded sagittal sections) with a dramatic reduction in the immunostaining for both E-cadherin and N-cadherin compared to control lenses, indicating impairment of cell-cell junctional integrity under the deficiency of drebrin. Moreover, the drebrin cKO lenses revealed expression of α-smooth muscle actin in the E18.5 epithelium which is completely absent in the control lenses (Fig. 7F, arrows). This latter finding together with loss of E-cadherin and the disruption of ZO-1 distribution indicates disruption of the epithelial phenotype and initiation of trans differentiation of epithelial cells into α-smooth muscle actin expressing myofibroblasts under the absence of drebrin. Images shown in Fig. 7 are representative of four biological replicates.

2.5. Drebrin deficiency impairs lens epithelial proliferation and survival

Having found a dramatic reduction in lens size, microphthalmia, and an abnormal lens epithelial phenotype in drebrin cKO mice, we evaluated for a plausible impairment in lens epithelial proliferation and cell survival under the absence of drebrin. For this, we performed a quantitative analysis of nuclei number in both the lens epithelium and fiber mass based on propidium iodide staining, TUNEL positive cells to score for apoptotic cell death, and Ki-67 positive nuclei to identify proliferating cells in sagittal cryosections from E18.5 and P1 drebrin cKO and control mouse lenses. Enumeration revealed a significant decrease in propidium iodide-stained nuclei in the lens epithelium and fiber mass of drebrin cKO lenses by ~80% and ~70%, respectively, compared to the corresponding controls (Fig. 8A and B). TUNEL labeling (green fluorescence) for apoptotic cells showed a significant increase in TUNEL positive cells (indicated with arrows) in both epithelium and fiber cells of the drebrin cKO mouse lenses (E18.5) compared to control lenses, indicating increased cell death under the absence of drebrin in the lens (Fig. 8C and D). Finally, immunostaining analysis of cryosections from drebrin cKO P1 mouse lenses for Ki-67, a marker of cell proliferation, revealed a significant decrease (~80%) in the number of Ki-67 positive cells in the epithelium, compared to the respective control lenses (Fig. 8E and F), which exhibited a relatively much higher number of Ki-67 positive cells in the equatorial epithelium (Fig. 8E,

arrow) relative to the central epithelium (Fig. 8E, arrowhead). The inserts in Figs. 8C and E show a magnified area of epithelium indicated with square boxes. Collectively, the analysis of these parameters implicates impaired lens epithelial proliferation and increased cell death in the decreased lens size found in the drebrin cKO mice.

2.6. Absence of drebrin disrupts lens fiber cell organization

Lens fiber cell differentiation was evident under the absence of drebrin as confirmed by the presence of fibers expressing differentiation-specific marker proteins including aquaporin-0 (APQ0), γ-crystallin and NrCAM in drebrin cKO mice (P1), refer to Fig. 9. However, fiber cell organization was clearly disrupted in drebrin cKO lenses relative to control lenses. Starting from E13.5, lens fiber cell orientation was found to be abnormal, with P1 lenses exhibiting gross distortion and impairment of secondary fiber cell suture formation (arrows, Fig. 9C) suggesting defects in fiber cell migration and cell-cell junctions under the absence of drebrin (Figs. 6 and 9). Moreover, as described earlier (Fig. 7), the drebrin cKO lenses revealed disruptions in ZO-1 organization and fulcrum establishment which play a crucial role(s) in maintaining polarity, anterior to posterior alignment, and migration pattern of lens fiber cells.[51]

3. DISCUSSION

This study explored the role of drebrin, a multifunctional cytoskeletal regulator in lens morphogenesis and growth. The ocular lens, which is a simple and transparent organ, has been considered as a model system to interrogate mechanistic aspects of developmental biology in general.[1] The Le-Cre transgenic mouse used to create a drebrin cKO mouse model in this study has been shown to express Cre recombinase prior to lens vesicle formation, and starting from day E8.75.[52] The drebrin cKO mouse lens was found to exhibit abnormalities starting at E13.5 indicating that drebrin might not be required for the lens vesicle formation, separation, or initiation of lens fiber cell differentiation. However, starting from E13.5, drebrin cKO lenses exhibited progressive growth defects, epithelial phenotype abnormalities, and fiber cell disorganization and degeneration, leading to microphathalmic eyes in affected animals by the pre-weanling stage. These phenotypes were evident even in drebrin haploinsufficient lenses suggesting that the normal expression of drebrin and its actin-associated cellular activities are a requirement for lens morphogenesis, growth, and architecture. To the best of our knowledge, there have been no prior studies illuminating a vital role for drebrin in lens development and growth.

The lens is developed from a single cell type consisting of the epithelial cells, during the differentiation of which, cells at the equatorial zone elongate and differentiate into long ribbon-like secondary fiber cells constituting the bulk of the organ in the adult eye.[6] Lens epithelial apical-basal elongation, polarity, and cell adhesive interactions, and fiber cell polarity, migration, hexagonal geometry, and compaction, which are critical for normal lens morphogenesis, growth, and architecture, are in turn dependent on the integrity of actin cytoskeletal and actomyosin organization, and cell adhesive interactions.[1, 3, 5, 51] Drebrin, which belongs to the superfamily of actin-depolymerizing factor homology (ADF-H) proteins, and couples actin filaments to microtubules,[26, 38, 39] has been demonstrated to

regulate neuronal development, dendritic spine morphogenesis, synaptic function, migration, spermatogenesis, and myoblast differentiation through its actin-binding and F-actin bundling activities.[23, 28, 38, 53] The predominant isoform of drebrin expressed in the lens is drebrin E, known to be expressed in various other non-neuronal tissues.[23, 24, 37] Interestingly, drebrin expression was found to be downregulated in a maturation-dependent manner in the mouse lens, with almost no protein being detected in mature (three-month-old mice) lenses, indicating that a key role for drebrin in the developing and differentiating but not the mature lens. This conclusion was also further supported by the developmental phenotype recorded in the drebrin cKO mouse lenses.

The distribution pattern of drebrin appears to be very similar to that of actin in both the epithelium and fibers, with evidence for colocalization of the proteins throughout the lens. Drebrin is phosphorylated by CDK5 and plays an important role in epithelial cell apical-basal elongation.[32, 37] In the lens epithelium, drebrin was distributed at both the apical and basal regions and the lateral side of the plasma membrane. Significantly, the drebrin cKO lens epithelium reveals abnormalities very similar to those we have previously observed in mouse models with impairments in molecular mechanisms regulating actin cytoskeletal dynamics in the lens. These include alterations in epithelial apical-basal height and sheet length, E-cadherin-based junctions, and induction of epithelial to mesenchymal transdifferentiation,[13, 17] further confirming the importance of proteins including drebrin that regulate actin cytoskeletal organization and actin dynamics in maintaining the lens epithelial phenotype. What is surprising about drebrin is that unlike many other prominently expressed cytoskeletal and cytoskeleton interacting proteins in the lens,[1, 5] even haploinsufficiency of the protein results in impairment of lens morphogenesis and growth, indicating an absolute requirement for normal levels of drebrin expression in lens development and growth.

The prominent phenotype found in the drebrin cKO mouse eye included a markedly reduced size of the eye and lens, and the fusion of lens with the cornea, iris, and lack of an established iridocorneal angle. Although Pax6 P0 enhancer/promoter-driven Cre recombinase expression is prominent in the lens of the Le-Cre mouse, Cre recombinase has also been reported to be expressed in other tissues of the eye anterior chamber.[52] Whether the deletion of drebrin expression in the iris, presumptive ciliary muscle, and trabecular meshwork and cornea played a role in the observed abnormalities of the anterior chamber tissues is debatable but we could not confirm or rule out this possibility because drebrin expression in other eye anterior segment tissues was very low relative to the lens and retina, in wild type mice. Lens developmental defects have been found to be commonly associated with microphthalmia as seen with the drebrin cKO mice in our study.[1, 6, 9] This is largely due to the developmental dependence of other ocular tissues on the growth-promoting factors produced and secreted by the lens.[6] In the drebrin cKO lens, the increased cell death due to enhanced apoptosis together with decreased epithelial proliferation and degeneration of fiber cells could be responsible in part, for the observed growth and size defects in the lens.

Unlike the lens growth and epithelial defects recorded in the absence of drebrin, lens fiber cell differentiation per se was not adversely impacted, based on the formation of both

primary and secondary fibers and the expression of fiber specific proteins in the cKO mouse lens. The absence of drebrin however, impaired establishment of fiber cell polarity based on the overt defects noticed in the establishment of apical junctions with epithelial cells and fulcrum, and alterations in the distribution profile of ZO-1, N-cadherin, actin, spectrin, and N-cadherin. Additionally, fiber cell orientation and migration pattern which are critical for the establishment of lens sutures and compaction were found to be defective in drebrin cKO lenses, confirming the importance of drebrin-regulated actin cytoskeletal dynamics and associated cellular processes for lens architecture and growth. Due to the severe and progressive degeneration of lens fibers in drebrin cKO mice, our ability to examine fiber cell hexagonal geometry, fiber cell-cell junctions, gap junction organization, and the membrane skeleton organization has been hampered.

In conclusion, this study uncovers a requirement for drebrin, an actin-binding protein in lens morphogenesis, and growth. Importantly, the absence of drebrin impairs lens epithelial phenotype, proliferation, polarity and survival, and fiber cell orientation and organization, collectively leading to defective lens morphogenesis, growth, integrity, and microphthalmia.

4. EXPERIMENTAL PROCEDURES

4.1 Mice

Mice used in this study were maintained in a pathogen-free vivarium under a 12-hour dark and light cycle with ad libitum food and water. All experiments using mice were carried out in accordance with the recommendations of the Guide for the Care and Use of Laboratory Animals of the National Institutes of Health and the Association for Research in Vision and Ophthalmology. The protocol (A213-19-10) was approved by the Institutional Animal Care and Use Committee (IACUC) of the Duke University School of Medicine.

4.2 Generation of the drebrin conditional knockout mouse model

The drebrin cKO mouse model was developed by mating drebrin floxed mice (with loxP sites flanking coding exons 3–8 of the *DBN1* gene; maintained on C57BL/6J background),[44] with lens-specific Cre recombinase expressing transgenic mice (Le-Cre mouse model) as described earlier.[13] The Le-Cre transgenic mice used in this study express Cre recombinase at embryonic day 8.75 under the control of a Pax6 P0 enhancer/promoter, with Cre being expressed in the lens epithelium and fiber cells as well as in other surface ectoderm-derived eye structures.[45, 52] For comparative analyses, drebrin cKO mice (generation F7 and above) were compared to littermate drebrin floxed controls that were negative for the Cre transgene. Tail DNA derived from the respective groups of animals was screened for drebrin floxed alleles and the Cre transgene by PCR using the following oligonucleotide primers.

Mouse *DBN1* forward: GGCTCTGTACACATACGAGGATGGCTCAGAT

Mouse *DBN1* reverse: AGTTGATGAGCACATATTTTGGCAGGGCAGCT

Cre primers: forward: GCATTACCGGTCGATGCAACGAGTGATGAG, and reverse

GAGTGAACGAACCTGGTCGAAATCAGTGCG.

Pregnant dams were anesthetized, and fetuses were extracted by hysterectomy at the appropriate gestational ages.

4.3 RT-PCR

To determine the relative expression level of drebrin isoforms (A and E) in mouse lens, total RNA was extracted from pooled neonatal (P2) and adult (P30) mouse lenses using a RNeasy Micro kit (Cat. No. 74004; Qiagen, Inc., Valencia, CA, USA) and reverse transcribed using the Advantage RT-for-PCR Kit (Cat. No. 639506; Takara Bio USA, Inc., Mountain View, CA, USA). Isoform-specific oligonucleotide PCR primers of *DBN1*:

(Drebrin A: forward-5'-AACTCGAGGCATGGCCGGCGTCAGCTTCAGCG-3', reverse-5'-AGGGATCCTTACCCCACCCTGCCGAGGCCT-3'.

Drebrin E: forward-5'-ATCTCCAGGGCTTGCTGCAGGTGAGGTGTG-3', reverse-5'-GGCACCCAGCACTTGGGATGCAGTGTCAGG-3') and Titanium® Taq PCR Kit (Cat no. 639210; Takara Bio USA, Inc., Mountain View, CA, USA) were used to amplify the drebrin specific DNA products from the reverse-transcribed single-stranded cDNA. The DNA products were separated by agarose gel electrophoresis and visualized using Gel Red Nucleic Acid Stain (Cat. No. 41002; Biotium, Hayward, CA, USA) and viewed with Bio-Rad ChemiDoc™ Touch Imaging System; Hercules, CA. DNA products were sequenced to confirm identity.

4.4 Tissue Fixation and Sectioning

Embryonic (E11.5, E13.5, E16.5, E17.5, and E18.5), neonatal (P1), and postnatal (P21 and P30) mouse eyes were fixed for cryostat or paraffin sectioning. For frozen tissue sectioning, embryonic heads (E11.5, E13.5, E16.5, E18.5, and P1) were fixed in 4% paraformaldehyde for 24 hours at 4 °C, and transferred into 5%, and 30% sucrose in PBS (phosphate-buffered saline) on successive days at 4 °C. Tissues were then embedded in optimal cutting temperature (OCT) media (Tissue-Tek, Torrance, CA, USA), and cut into 10-μm-thick sections (sagittal plane) using a Microm™ HM550 Cryostat (GMI, Ramsey, MN, USA) as described by us previously.[12]

For paraffin sections, tissue specimens (E17.5, P1, P21, and P30 mouse eyes) were fixed in 3.7% buffered formalin for 48 hours at room temperature, embedded in paraffin, and used to generate 5-μm-thick sections (both sagittal and equatorial plane) as we described earlier.[54]

4.5 Immunofluorescence and Imaging

Sagittal and equatorial plane sections derived from cryofixed and paraffin-embedded mouse eyes were used for immunofluorescence analyses. Paraffin tissue sections were deparaffinized and rehydrated using xylene and absolute ethyl alcohol, respectively, as we described earlier.[54] Specimens were then placed in preheated antigen retrieval solution (0.1 M sodium citrate buffer, pH 6.0) and heated for 20 minutes at 100 °C in a water bath. After rinsing, the tissue sections were blocked for 10 minutes in a humidified chamber using medical background Sniper reducing solution (Cat. No. BS966H; Biocare Medical, Concord, CA).

For paraffin sections, primary antibodies in Tris-buffered saline containing 1% bovine serum albumin were incubated overnight with tissue sections in a humidified chamber at 4 °C, either individually or in combination with other primary antibodies for double labeling (as described in Table 1).

Air-dried tissue cryosections were treated with Image-iT FX signal enhancer (Invitrogen, Eugene, OR, USA) and blocked using blocking buffer (5% globulin-free BSA and 5% filtered goat serum in 0.3% Triton X-100 containing PBS) for 30 minutes each. Primary antibodies (as described in Table 1) were added in blocking buffer and incubated with tissue sections overnight at 4 °C in a humidified chamber.

The slides were washed and incubated with either Alexa fluor 488 or 568 conjugated secondary antibodies (Invitrogen; at 1:500 dilution) or both (for double labeling) under dark conditions for 2 hours at room temperature. Slides were then washed and mounted using Vectashield® Antifade Mounting Medium (Cat. No: H-1000; Vector Laboratories, Burlingame, CA), with images being captured using a Nikon Eclipse 90i confocal laser scanning microscope. For all immunofluorescence analyses described in this study, a minimum of three independent specimens (biological replicates) was analyzed, with three serial sections from each specimen.

The fluorescence intensity of lens area in Figure 4E are analyzed and quantified using ImageJ software. The lens area in each image is specified using freehand ROI tool. For quantification, the mean pixel fluorescence value of the freehand ROI regions is used. It is defined as the sum of fluorescence values in the region normalized by its area. The mean pixel fluorescence value is measured using the analyze/measure tool. For images in all the groups, the lens region and background region (no fluorescence region) are selected. The mean pixel fluorescence values for both the lens region and background region are measured. The mean pixel fluorescence value of background region is then subtracted from that of the lens region. The graph is plotted with the mean fluorescence pixel intensity (in arbitrary units) per unit area of lens for all the groups.

To measure the change in lens epithelial cell height, the distance from the basal to apical regions of the epithelium was measured (in microns) using the measure/length tool in the images captured with Nikon Eclipse 90i confocal laser scanning microscope. Similarly, to measure the length of lens epithelial sheet, a line was drawn from the left to the right equatorial epithelial regions using a freehand ROI tool and the distance between these two regions was measured in microns using the measure/length tool.

4.6 Histological analysis

Embryonic heads (E13.5, and 18.5) and whole eyes (from postnatal P1, and P8 mice) were fixed for 48 hours at room temperature in 3.7% buffered formalin. Drebrin cKO and respective littermate control (drebrin floxed) specimens were subsequently dehydrated, embedded in paraffin, and cut in 5 μm thick sections with a rotary microtome (Leica Biosystems, Buffalo Grove, IL, USA). Tissue sections were deparaffinized and rehydrated using xylene and ethyl alcohol. Sections were immersed in Harris hematoxylin for 5 minutes and rinsed with water for 5 minutes. Sections were then stained with eosin for 2 minutes,

washed with water, and dehydrated with ethyl alcohol and xylene. Slides were mounted using Permount and air-dried at room temperature. Images were captured using Zeiss Axio Imager equipped with a Hamamatsu Orca ER monochrome CCD camera.

4.7 Immunoblotting

To analyze the distribution profile of drebrin in membrane rich and cytosolic fractions, whole lenses (P30) were dissected free of other tissue. Lens tissue (4–5 lenses/pooled sample) was homogenized using a Dounce glass homogenizer and cold (4 °C) hypotonic buffer containing 10 mM Tris buffer, pH 7.4, 0.2 mM MgCl2, 5 mM N-ethylmaleimide, 2 mM sodium orthovanadate, 10 mM sodium fluoride, 60 μM phenylmethylsulfonyl fluoride, 0.4 mM iodoacetamide, EDTA-free protease inhibitor cocktail and PhosSTOP phosphatase inhibitor cocktail (one tablet of each per 10 ml buffer; Roche, Manheim, Germany). Lysates were centrifuged at 800 × g for 20 minutes and the resulting supernatants further centrifuged at 100,000 × g for 1 hour at 4 °C using a Beckman tabletop ultracentrifuge. The pellets were suspended in a sample buffer containing 8 M urea, 20 mM Tris, 23 mM glycine, 0.5 M dithiothreitol, and saturated sucrose, further sonicated and used as the membrane-enriched fraction, while the supernatant was used as the cytosolic fraction. To determine changes in protein levels of drebrin in neonatal and postnatal lenses, and the distribution profile of drebrin in the lens epithelium and fiber mass, lens lysates were prepared in the hypotonic buffer and centrifuged at 800 × g for 20 minutes to derive supernatants for analysis.
To evaluate for the presence of drebrin A in the brain, P1 and P30 whole brains were homogenized in hypotonic buffer and centrifuged at 800 × g for 20 minutes to derive supernatants for analysis.

Protein concentration was determined in 800 × g supernatants of brain and lens, lens epithelium and fiber samples, and lens cytosolic fractions using the Pierce™ BCA Protein Assay Kit (Cat. No. 23225; Thermo Fisher Scientific). The protein concentration of membrane-enriched fractions was determined using the Pierce™ 660nm Protein Assay Reagent (Cat. No. 22660; Thermo Fisher Scientific). Thirty micrograms of protein from lens and brain cytosolic, membrane fractions and 800 × g supernatants were thoroughly mixed with freshly prepared 4x Laemmli buffer containing 40 mM dithiothreitol and boiled for 5 minutes at 100 °C. Protein samples were separated on 8% acrylamide gels and electrophoretically transferred to nitrocellulose membranes (Bio-Rad). Nitrocellulose membranes were probed with drebrin monoclonal antibody (Cat. No. BM5537; Origene Technologies Inc, Rockville, MD; Dilution 1:1000), Drebrin-A polyclonal antibody (Cat. No. 28023; Immuno-Biological Laboratories Co., Ltd. Gunma, Japan; Dilution 1:300) and subsequently with appropriate secondary antibody. GAPDH (Glyceraldehyde 3-phosphate dehydrogenase) (Cat. No. 60004-1; Proteintech Group, Chicago, IL; Dilution 1:5000) was immunoblotted as a loading control. Blots were developed by chemiluminescence using Chemidoc™ Touch (Bio-Rad), and protein bands were quantified using ImageJ Software.

4.8 TUNEL assay

To evaluate and compare apoptotic cell death in drebrin cKO and littermate control mouse lenses, embryonic E18.5 and P1 stage tissue cryosections were subjected to in-situ Terminal deoxynucleotidyl Transferase dUTP Nick End Labeling (TUNEL) using an ApopTag Plus

Fluorescein Kit (EMD Millipore, Burlington, MA, USA) as we described earlier.[12] TUNEL labeled tissue sections were counter-stained with propidium iodide. Imaging was performed using a Nikon Eclipse 90i confocal microscope in conjunction with manual counting of TUNEL positive cells.

4.9 Statistical analysis

Student's t-test was performed to determine the significance of differences ($P<0.05$) between data derived from control and drebrin cKO lens specimens. One-way analysis of variance with post hoc Holm-Sidak's multiple comparison test was used to compare between the groups. Values are represented as mean±SEM (standard error of the mean) of 4–10 samples.

ACKNOWLEDGMENTS

This work was supported by the National Institutes of Health grant-R01EY025096. We thank Ruth Ashery-Padan, Ph.D., for her generous permission to use the Le-Cre transgenic mice in this study. We also thank Samuel Zigler, Jr, Ph.D., from the Johns Hopkins University School of Medicine, Baltimore, MD., for γ-crystallin antibody, and Joseph Horwitz, Ph.D., from the Jules Stain Eye Institute, UCLA. CA., for aquaporin-0 antibody.

REFERENCES

1. Cvekl A, Zhang X. Signaling and Gene Regulatory Networks in Mammalian Lens Development. Trends Genet. 10 2017;33(10):677–702. doi:10.1016/j.tig.2017.08.001 [PubMed: 28867048]
2. Sugiyama Y, Prescott AR, Tholozan FM, Ohno S, Quinlan RA. Expression and localisation of apical junctional complex proteins in lens epithelial cells. Exp Eye Res. 7 2008;87(1):64–70. doi:10.1016/j.exer.2008.03.017 [PubMed: 18508048]
3. Rao PV. The pulling, pushing and fusing of lens fibers: a role for Rho GTPases. Cell Adh Migr. Jul-Sep 2008;2(3):170–3. doi:10.4161/cam.2.3.6495 [PubMed: 19262112]
4. Bassnett S, Shi Y, Vrensen GF. Biological glass: structural determinants of eye lens transparency. Philos Trans R Soc Lond B Biol Sci. 4 27 2011;366(1568):1250–64. doi:10.1098/rstb.2010.0302 [PubMed: 21402584]
5. Cheng C, Nowak RB, Fowler VM. The lens actin filament cytoskeleton: Diverse structures for complex functions. Exp Eye Res. 3 2017;156:58–71. doi:10.1016/j.exer.2016.03.005 [PubMed: 26971460]
6. Lovicu FJ, McAvoy JW. Growth factor regulation of lens development. Dev Biol. 4 1 2005;280(1):1–14. doi:10.1016/j.ydbio.2005.01.020 [PubMed: 15766743]
7. Song S, Landsbury A, Dahm R, Liu Y, Zhang Q, Quinlan RA. Functions of the intermediate filament cytoskeleton in the eye lens. J Clin Invest. 7 2009;119(7):1837–48. doi:10.1172/JCI38277 [PubMed: 19587458]
8. Hejtmancik JF, Riazuddin SA, McGreal R, Liu W, Cvekl A, Shiels A. Lens Biology and Biochemistry. Prog Mol Biol Transl Sci. 2015;134:169–201. doi:10.1016/bs.pmbts.2015.04.007 [PubMed: 26310155]
9. Chauhan B, Plageman T, Lou M, Lang R. Epithelial morphogenesis: the mouse eye as a model system. Curr Top Dev Biol. 2015;111:375–99. doi:10.1016/bs.ctdb.2014.11.011 [PubMed: 25662266]
10. Chauhan BK, Disanza A, Choi SY, et al. Cdc42- and IRSp53-dependent contractile filopodia tether presumptive lens and retina to coordinate epithelial invagination. Development. 11 2009;136(21):3657–67. doi:10.1242/dev.042242 [PubMed: 19820184]
11. Chauhan BK, Lou M, Zheng Y, Lang RA. Balanced Rac1 and RhoA activities regulate cell shape and drive invagination morphogenesis in epithelia. Proc Natl Acad Sci U S A. 11 8 2011;108(45):18289–94. doi:10.1073/pnas.1108993108 [PubMed: 22021442]

12. Maddala R, Chauhan BK, Walker C, et al. Rac1 GTPase-deficient mouse lens exhibits defects in shape, suture formation, fiber cell migration and survival. Dev Biol. 12 1 2011;360(1):30–43. doi:10.1016/j.ydbio.2011.09.004 [PubMed: 21945075]
13. Maddala R, Nagendran T, Lang RA, Morozov A, Rao PV. Rap1 GTPase is required for mouse lens epithelial maintenance and morphogenesis. Dev Biol. 10 1 2015;406(1):74–91. doi:10.1016/j.ydbio.2015.06.022 [PubMed: 26212757]
14. Maddala R, Reneker LW, Pendurthi B, Rao PV. Rho GDP dissociation inhibitor-mediated disruption of Rho GTPase activity impairs lens fiber cell migration, elongation and survival. Dev Biol. 3 1 2008;315(1):217–31. doi:10.1016/j.ydbio.2007.12.039 [PubMed: 18234179]
15. Nowak RB, Fischer RS, Zoltoski RK, Kuszak JR, Fowler VM. Tropomodulin1 is required for membrane skeleton organization and hexagonal geometry of fiber cells in the mouse lens. J Cell Biol. 9 21 2009;186(6):915–28. doi:10.1083/jcb.200905065 [PubMed: 19752024]
16. Rao PV, Maddala R. The role of the lens actin cytoskeleton in fiber cell elongation and differentiation. Semin Cell Dev Biol. 12 2006;17(6):698–711. doi:10.1016/j.semcdb.2006.10.011 [PubMed: 17145190]
17. Rasiah PK, Maddala R, Bennett V, Rao PV. Ankyrin-G regulated epithelial phenotype is required for mouse lens morphogenesis and growth. Dev Biol. 2 1 2019;446(1):119–131. doi:10.1016/j.ydbio.2018.12.016 [PubMed: 30562487]
18. Korol A, Taiyab A, West-Mays JA. RhoA/ROCK signaling regulates TGFbeta-induced epithelial-mesenchymal transition of lens epithelial cells through MRTF-A. Mol Med. 12 2016;22:713–723. doi:10.2119/molmed.2016.00041 [PubMed: 27704140]
19. Shibata T, Shibata S, Ishigaki Y, et al. Tropomyosin 2 heterozygous knockout in mice using CRISPR-Cas9 system displays the inhibition of injury-induced epithelial-mesenchymal transition, and lens opacity. Mech Ageing Dev. 4 2018;171:24–30. doi:10.1016/j.mad.2018.03.001 [PubMed: 29510160]
20. Maddala R, Mongan M, Xia Y, Rao PV. Calponin-3 deficiency augments contractile activity, plasticity, fibrogenic response and Yap/Taz transcriptional activation in lens epithelial cells and explants. Sci Rep. 1 28 2020;10(1):1295. doi:10.1038/s41598-020-58189-y [PubMed: 31992794]
21. Kakrana A, Yang A, Anand D, et al. iSyTE 2.0: a database for expression-based gene discovery in the eye. Nucleic Acids Res. 1 4 2018;46(D1):D875–D885. doi:10.1093/nar/gkx837 [PubMed: 29036527]
22. Maddala RGJ, Mathais RT, et al. . Absence of S100A4 in the mouse lens induces an aberrant retina-specific differentiation program and cataract. Sci Rep. 2020:In press.
23. Shirao T, Hanamura K, Koganezawa N, Ishizuka Y, Yamazaki H, Sekino Y. The role of drebrin in neurons. J Neurochem. 6 2017;141(6):819–834. doi:10.1111/jnc.13988 [PubMed: 28199019]
24. Peitsch WK, Grund C, Kuhn C, et al. Drebrin is a widespread actin-associating protein enriched at junctional plaques, defining a specific microfilament anchorage system in polar epithelial cells. Eur J Cell Biol. 11 1999;78(11):767–78. doi:10.1016/S0171-9335(99)80027-2 [PubMed: 10604653]
25. Li MW, Xiao X, Mruk DD, et al. Actin-binding protein drebrin E is involved in junction dynamics during spermatogenesis. Spermatogenesis. Apr-Jun 2011;1(2):123–136. doi:10.4161/spmg.1.2.16393 [PubMed: 22319661]
26. Geraldo S, Khanzada UK, Parsons M, Chilton JK, Gordon-Weeks PR. Targeting of the F-actin-binding protein drebrin by the microtubule plus-tip protein EB3 is required for neuritogenesis. Nat Cell Biol. 10 2008;10(10):1181–9. doi:10.1038/ncb1778 [PubMed: 18806788]
27. Grintsevich EE. Remodeling of Actin Filaments by Drebrin A and Its Implications. Adv Exp Med Biol. 2017;1006:61–82. doi:10.1007/978-4-431-56550-5_5 [PubMed: 28865015]
28. Hayashi K Cell Shape Change by Drebrin. Adv Exp Med Biol. 2017;1006:83–101. doi:10.1007/978-4-431-56550-5_6 [PubMed: 28865016]
29. Hayashi K, Ishikawa R, Ye LH, et al. Modulatory role of drebrin on the cytoskeleton within dendritic spines in the rat cerebral cortex. J Neurosci. 11 15 1996;16(22):7161–70. [PubMed: 8929425]

30. Ishikawa R, Hayashi K, Shirao T, et al. Drebrin, a development-associated brain protein from rat embryo, causes the dissociation of tropomyosin from actin filaments. J Biol Chem. 11 25 1994;269(47):29928–33. [PubMed: 7961990]

31. Mikati MA, Grintsevich EE, Reisler E. Drebrin-induced stabilization of actin filaments. J Biol Chem. 7 5 2013;288(27):19926–38. doi:10.1074/jbc.M113.472647 [PubMed: 23696644]

32. Worth DC, Daly CN, Geraldo S, Oozeer F, Gordon-Weeks PR. Drebrin contains a cryptic F-actin-bundling activity regulated by Cdk5 phosphorylation. J Cell Biol. 9 2 2013;202(5):793–806. doi:10.1083/jcb.201303005 [PubMed: 23979715]

33. Kubota H, Ishikawa R, Ohki T, Ishizuka J, Mikhailenko SV, Ishiwata S. Modulation of the mechano-chemical properties of myosin V by drebrin-E. Biochem Biophys Res Commun. 10 1 2010;400(4):643–8. doi:10.1016/j.bbrc.2010.08.120 [PubMed: 20816663]

34. Hilton DM, Aguilar RM, Johnston AB, Goode BL. Species-Specific Functions of Twinfilin in Actin Filament Depolymerization. J Mol Biol. 9 14 2018;430(18 Pt B):3323–3336. doi:10.1016/j.jmb.2018.06.025 [PubMed: 29928893]

35. Yamazaki H, Shirao T. Homer, Spikar, and Other Drebrin-Binding Proteins in the Brain. Adv Exp Med Biol. 2017;1006:249–268. doi:10.1007/978-4-431-56550-5_14 [PubMed: 28865024]

36. Butkevich E, Hulsmann S, Wenzel D, Shirao T, Duden R, Majoul I. Drebrin is a novel connexin-43 binding partner that links gap junctions to the submembrane cytoskeleton. Curr Biol. 4 20 2004;14(8):650–8. doi:10.1016/j.cub.2004.03.063 [PubMed: 15084279]

37. Bazellieres E, Massey-Harroche D, Barthelemy-Requin M, Richard F, Arsanto JP, Le Bivic A. Apico-basal elongation requires a drebrin-E-EB3 complex in columnar human epithelial cells. J Cell Sci. 2 15 2012;125(Pt 4):919–31. doi:10.1242/jcs.092676 [PubMed: 22275434]

38. Ketschek A, Spillane M, Dun XP, Hardy H, Chilton J, Gallo G. Drebrin coordinates the actin and microtubule cytoskeleton during the initiation of axon collateral branches. Dev Neurobiol. 10 2016;76(10):1092–110. doi:10.1002/dneu.22377 [PubMed: 26731339]

39. Trivedi N, Stabley DR, Cain B, et al. Drebrin-mediated microtubule-actomyosin coupling steers cerebellar granule neuron nucleokinesis and migration pathway selection. Nat Commun. 2 23 2017;8:14484. doi:10.1038/ncomms14484 [PubMed: 28230156]

40. Rehm K, Panzer L, van Vliet V, Genot E, Linder S. Drebrin preserves endothelial integrity by stabilizing nectin at adherens junctions. J Cell Sci. 8 15 2013;126(Pt 16):3756–69. doi:10.1242/jcs.129437 [PubMed: 23750010]

41. Dart AE, Gordon-Weeks PR. The Role of Drebrin in Cancer Cell Invasion. Adv Exp Med Biol. 2017;1006:375–389. doi:10.1007/978-4-431-56550-5_23 [PubMed: 28865033]

42. Ivanov A, Esclapez M, Ferhat L. Role of drebrin A in dendritic spine plasticity and synaptic function: Implications in neurological disorders. Commun Integr Biol. 5 2009;2(3):268–70. doi:10.4161/cib.2.3.8166 [PubMed: 19641748]

43. Sekino Y, Koganezawa N, Mizui T, Shirao T. Role of Drebrin in Synaptic Plasticity. Adv Exp Med Biol. 2017;1006:183–201. doi:10.1007/978-4-431-56550-5_11 [PubMed: 28865021]

44. Zhang L, Wu JH, Huang TQ, et al. Drebrin regulates angiotensin II-induced aortic remodelling. Cardiovasc Res. 11 1 2018;114(13):1806–1815. doi:10.1093/cvr/cvy151 [PubMed: 29931051]

45. Ashery-Padan R, Marquardt T, Zhou X, Gruss P. Pax6 activity in the lens primordium is required for lens formation and for correct placement of a single retina in the eye. Genes Dev. 11 1 2000;14(21):2701–11. doi:10.1101/gad.184000 [PubMed: 11069887]

46. Takahashi H, Sekino Y, Tanaka S, Mizui T, Kishi S, Shirao T. Drebrin-dependent actin clustering in dendritic filopodia governs synaptic targeting of postsynaptic density-95 and dendritic spine morphogenesis. J Neurosci. 7 23 2003;23(16):6586–95. [PubMed: 12878700]

47. Nielsen PA, Baruch A, Shestopalov VI, et al. Lens connexins alpha3Cx46 and alpha8Cx50 interact with zonula occludens protein-1 (ZO-1). Mol Biol Cell. 6 2003;14(6):2470–81. doi:10.1091/mbc.e02-10-0637 [PubMed: 12808044]

48. Pontoriero GF, Smith AN, Miller LA, Radice GL, West-Mays JA, Lang RA. Co-operative roles for E-cadherin and N-cadherin during lens vesicle separation and lens epithelial cell survival. Dev Biol. 2 15 2009;326(2):403–17. doi:10.1016/j.ydbio.2008.10.011 [PubMed: 18996109]

49. Logan CM, Rajakaruna S, Bowen C, Radice GL, Robinson ML, Menko AS. N-cadherin regulates signaling mechanisms required for lens fiber cell elongation and lens morphogenesis. Dev Biol. 8 1 2017;428(1):118–134. doi:10.1016/j.ydbio.2017.05.022 [PubMed: 28552735]

50. More MI, Kirsch FP, Rathjen FG. Targeted ablation of NrCAM or ankyrin-B results in disorganized lens fibers leading to cataract formation. J Cell Biol. 7 9 2001;154(1):187–96. doi:10.1083/jcb.200104038 [PubMed: 11449000]

51. Sugiyama Y, Akimoto K, Robinson ML, Ohno S, Quinlan RA. A cell polarity protein aPKClambda is required for eye lens formation and growth. Dev Biol. 12 15 2009;336(2):246–56. doi:10.1016/j.ydbio.2009.10.010 [PubMed: 19835853]

52. Lam PT, Padula SL, Hoang TV, et al. Considerations for the use of Cre recombinase for conditional gene deletion in the mouse lens. Hum Genomics. 2 15 2019;13(1):10. doi:10.1186/s40246-019-0192-8 [PubMed: 30770771]

53. Krauss RS. Regulation of Skeletal Myoblast Differentiation by Drebrin. Adv Exp Med Biol. 2017;1006:361–373. doi:10.1007/978-4-431-56550-5_22 [PubMed: 28865032]

54. Karnam S, Skiba NP, Rao PV. Biochemical and biomechanical characteristics of dystrophin-deficient mdx(3cv) mouse lens. Biochim Biophys Acta Mol Basis Dis. 10 27 2020;1867(1):165998. doi:10.1016/j.bbadis.2020.165998 [PubMed: 33127476]

Key findings

- Drebrin E distributes to the lens epithelium and fibers and is downregulated in the mature lenses.
- Conditional deficiency of drebrin impairs lens morphogenesis, leading to microphthalmia.
- Drebrin deficiency affects lens epithelial phenotype, proliferation, and survival.
- Drebrin deficiency disrupts lens fiber cell polarity, organization, and adhesion.

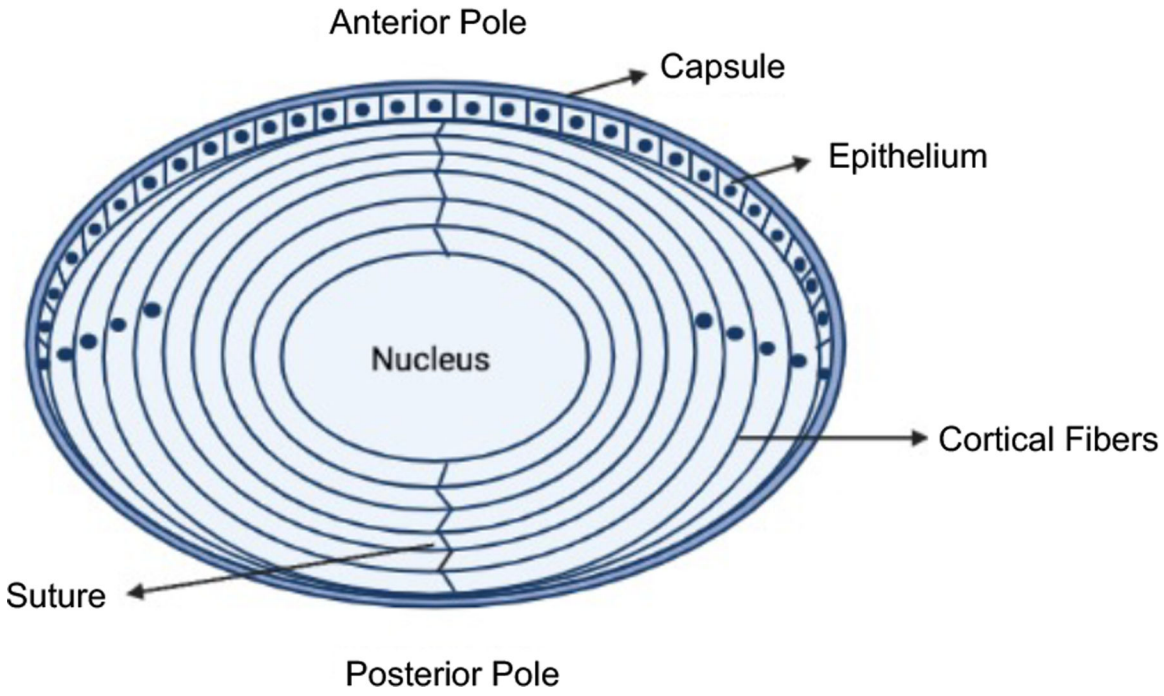

Fig. 1:
A schematic illustration of lens structure.

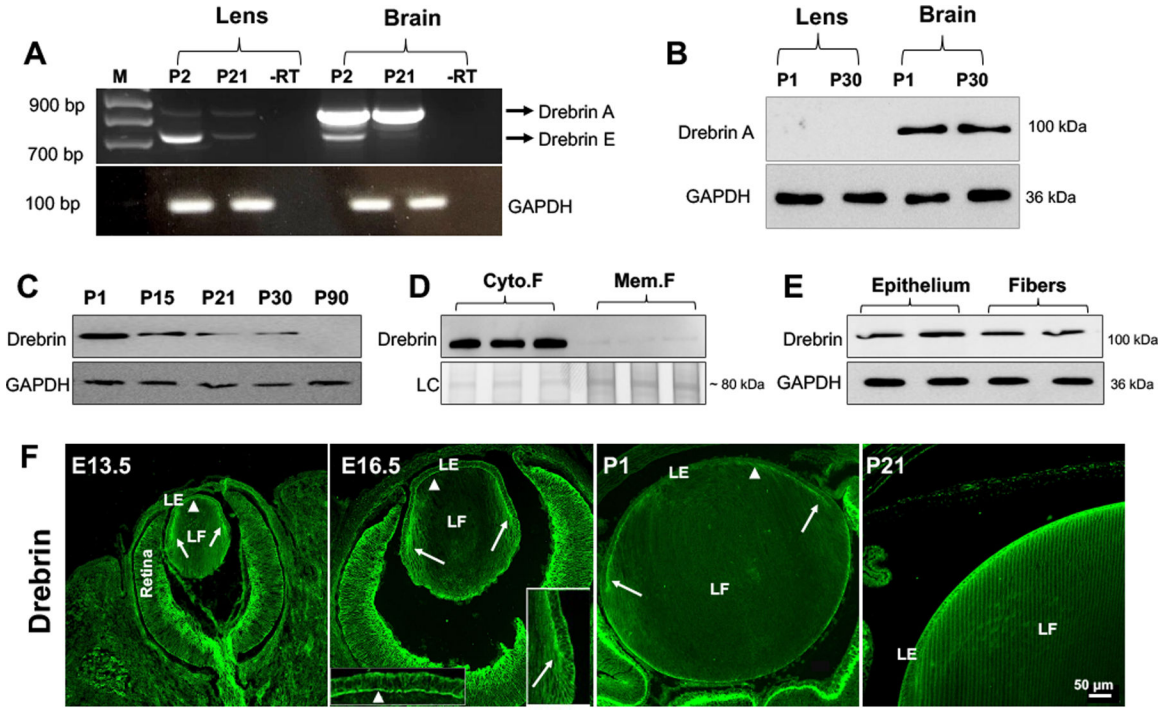

Figure 2: The expression and distribution profile of drebrin E in the mouse lens.

A) RT-PCR analysis of P2 and P21 mouse lenses and brain. The GAPDH DNA product confirms the normalization of a single-stranded cDNA used from the P2 and P21 specimens. **B)** Immunoblotting-based detection of drebrin A in P1 and P30 mouse lens and brain lysates. **C)** Immunoblotting of drebrin in P1, P15, P21, P30, and P90 mouse lenses. **D)** Immunoblotting of drebrin in the cytosolic and membrane-enriched fractions of P30 lenses. For cytosolic and membrane fractions, protein samples from the respective fractions separated on SDS-PAGE were stained with Gelcode blue with the staining intensity of the indicated protein band used as a loading control (LC). Data are shown for three biological replicates. Cyto.F: Cytoplasmic fraction, Mem.F: Membrane fraction. **E)** Immunoblotting analysis of drebrin in P1 mouse lens epithelial and fiber fractions showing drebrin distribution in both fractions. **F)** Immunofluorescence-based analysis of E13.5, E16.5, and P1 mouse lens cryosections revealed relatively intense distribution of drebrin at the apical-apical junctions of lens epithelial and fiber cells (arrowheads) and the lens fulcrum (arrows). Inserts show magnified areas of apical-apical junctions at the central and equatorial epithelial regions of the lens. In P21 lenses (paraffin section), drebrin expression is evident in both epithelial and fiber cells. LE: Lens epithelium, LF: Lens fibers. Scale bar; Image magnification. In panels B-E, GAPDH was immunoblotted as a loading control.

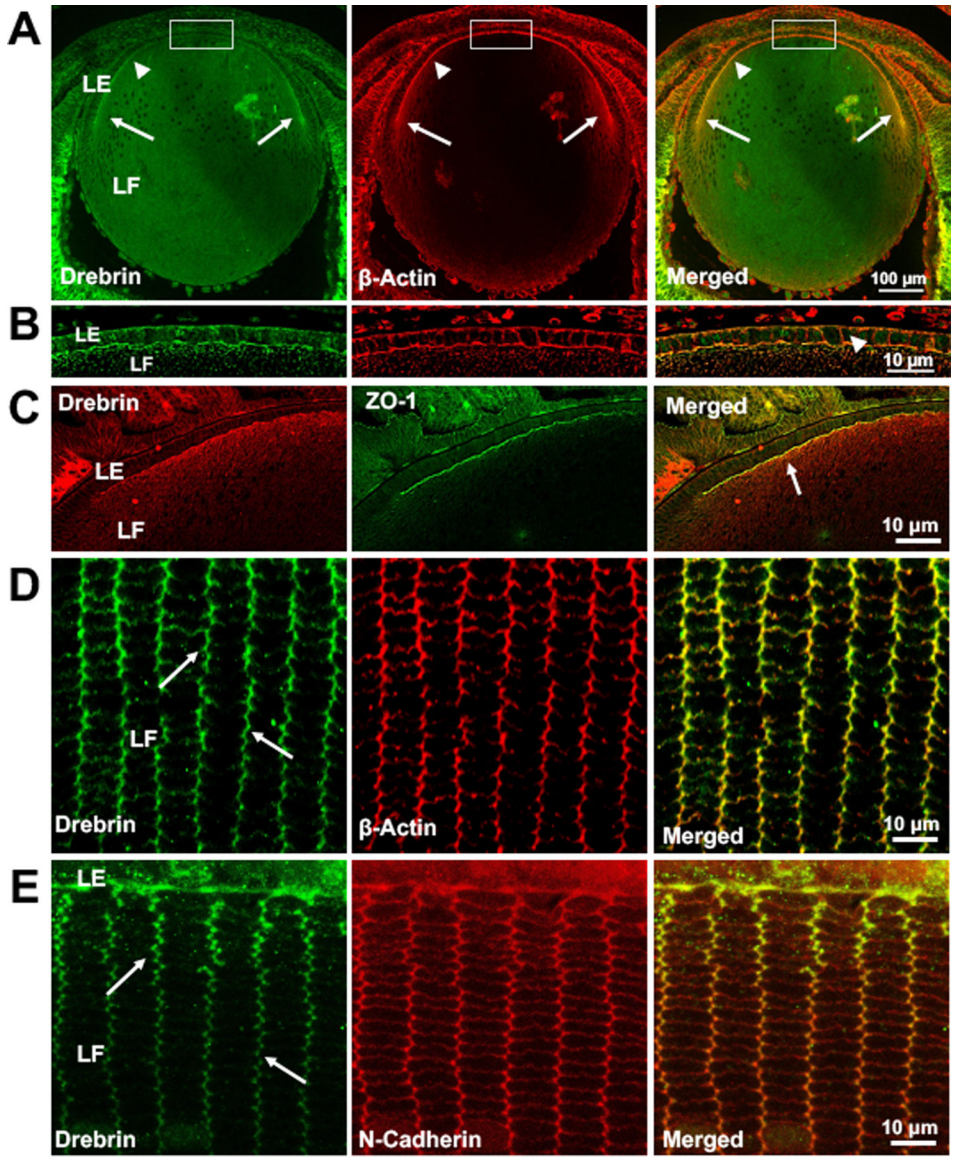

Figure 3: Distribution and colocalization of drebrin with β-actin and cell adhesion proteins in the mouse lens.

A) Immunofluorescence-based analysis of sagittal paraffin-embedded sections from the E17.5 eyeball, exhibiting co-localization of drebrin and β-actin at the apical-apical junctions of lens epithelial and fiber cells (arrowheads), and the lens fulcrum region (arrows). **B)** Enlarged images of the area boxed in panel A shows distribution and colocalization of drebrin with β-actin at the basal and apical regions, and to the lateral membrane of the lens epithelium (arrowheads). **C)** P1 sagittal paraffin-embedded sections of the lens showing co-localization of drebrin with ZO-1 (immunofluorescence, arrows). **D)** Equatorial lens sections derived from P30 mice reveal that drebrin distributes intensely at the vertices (arrows) of hexagonal fiber cells similar to the pattern exhibited by β-actin, and colocalizes with β-actin as evidenced by immunofluorescence analysis. Images were taken from the cortical region of the lens (50 μm from the epithelium). **E**) Drebrin exhibits colocalization with N-cadherin at the vertices of hexagonal lens fibers of the P30 mouse based on

immunofluorescence analysis. Images were captured from the outer cortical region of the lens. LE: Lens epithelium, LF: Lens fibers. Scale bars; Image magnification.

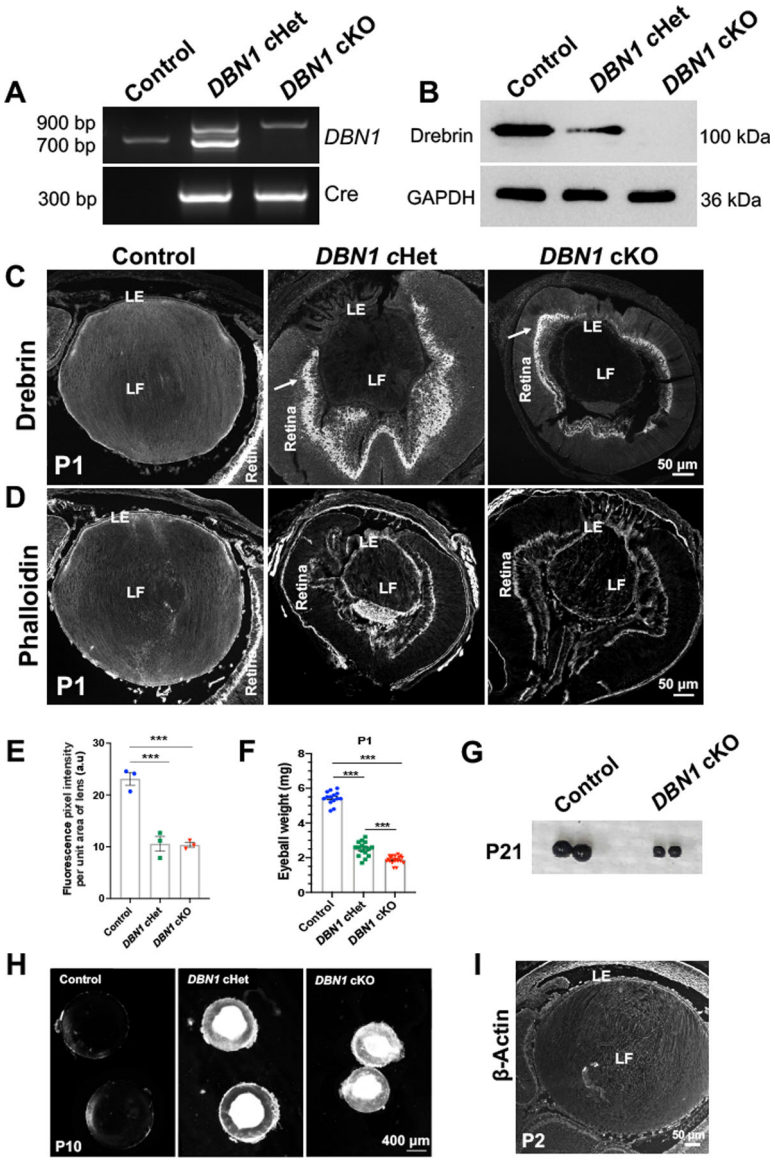

Figure 4: Impaired lens morphogenesis, cataract formation and microphthalmia in the drebrin conditional deficient mouse.

A) PCR based genotyping of drebrin (*DBN1*)/Le-Cre conditional mutant mice. **B**) Immunoblotting analysis confirming the deficiency of drebrin by > 99% and ~60% in P1 *DBN1* cKO and cHet mouse lenses, respectively, relative to littermate control (floxed) mice. GAPDH was immunoblotted as a loading control. **C)** Immunofluorescence analysis of P1 lens cryosections derived from the *DBN1* cHet and cKO mice revealed much reduced and undetectable drebrin staining, respectively, compared to control lenses. In contrast, expression of drebrin in the retina (arrow) of drebrin cHet and cKO mice was not suppressed. **D**) Eyes derived from the *DBN1* cHet and cKO P1 mice reveal an overt phenotype including markedly reduced lens size and abnormal lens shape along with significantly reduced staining for actin. **E**) Immunofluorescence quantification of rhodamine-phalloidin staining (n=3) compared to controls. **F**) A significant decrease in eyeball-wet weight was noted in P1 *DBN1* cHet (~54%) and cKO (~65%) mice relative to

control eyes. **G**) Representative images of the microphthalmic eyes of P21 *DBN1* cKO mice (>F7 generation) and control mice. **H)** Representative images of cataractous lenses of P10 cHet and cKO drebrin mice compared to transparent lenses from control mice. **I)** P2 Le-Cre transgenic mouse lens exhibits a normal morphology (stained for β-actin) comparable to control lens. The data in panel **F** represent mean±SEM of >10 biological replicates. ***P < 0.001. LE: Lens epithelium, LF: Lens fibers. Scale bar; Image magnification.

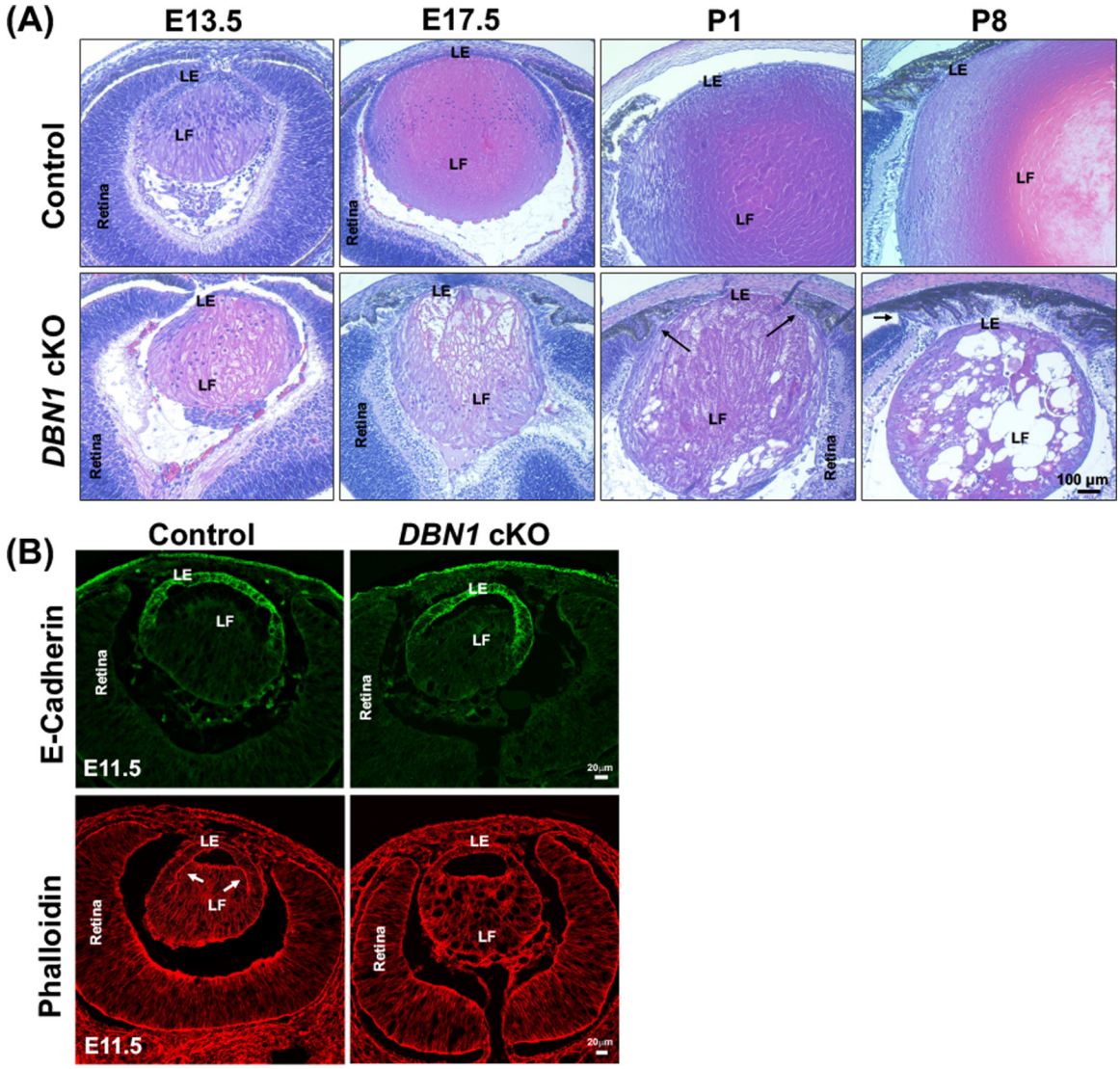

Figure 5: Drebrin cKO mouse lenses reveal progressive and extensive histological abnormalities.

A) To evaluate drebrin deficiency-induced effects on lens morphogenesis and integrity, paraffin-embedded sections (sagittal plane) derived from E13.5, E17.5, P1, and P8 *DBN1* cKO and littermate control (floxed) mouse eyes were stained with hematoxylin and eosin for histological analysis. Representative images are shown to depict the progressive histological changes in lens integrity at different stages from E13.5 to P8. Starting at stage E13.5, abnormalities were recorded in lens shape, size, fiber cell organization, and nuclei distribution in the fibers of drebrin cKO specimens, together with accumulation of large vacuoles and gross degeneration of fibers in the P8 drebrin cKO mouse lens compared to those from control mice. Additionally, as can be seen in the P1 and P8 drebrin cKO specimens, there is a fusion of the iris and lens with the cornea along with a lack of a well-developed iridocorneal angle (arrows) compared to control specimens. Scale bar; Image magnification. **B)** To assess the effects of drebrin deficiency on lens epithelium and primary fiber cell elongation, cryosections derived from the E11.5 cKO drebrin and littermate control mouse eye specimens (sagittal section) were stained for E-cadherin and F-actin. The E11.5

cKO drebrin mouse lens exhibits a normal epithelial phenotype similar to control lens based on E-cadherin distribution whereas development of the fulcrum in the drebrin deficient lens appears to be impaired compared to the control lens (arrow).

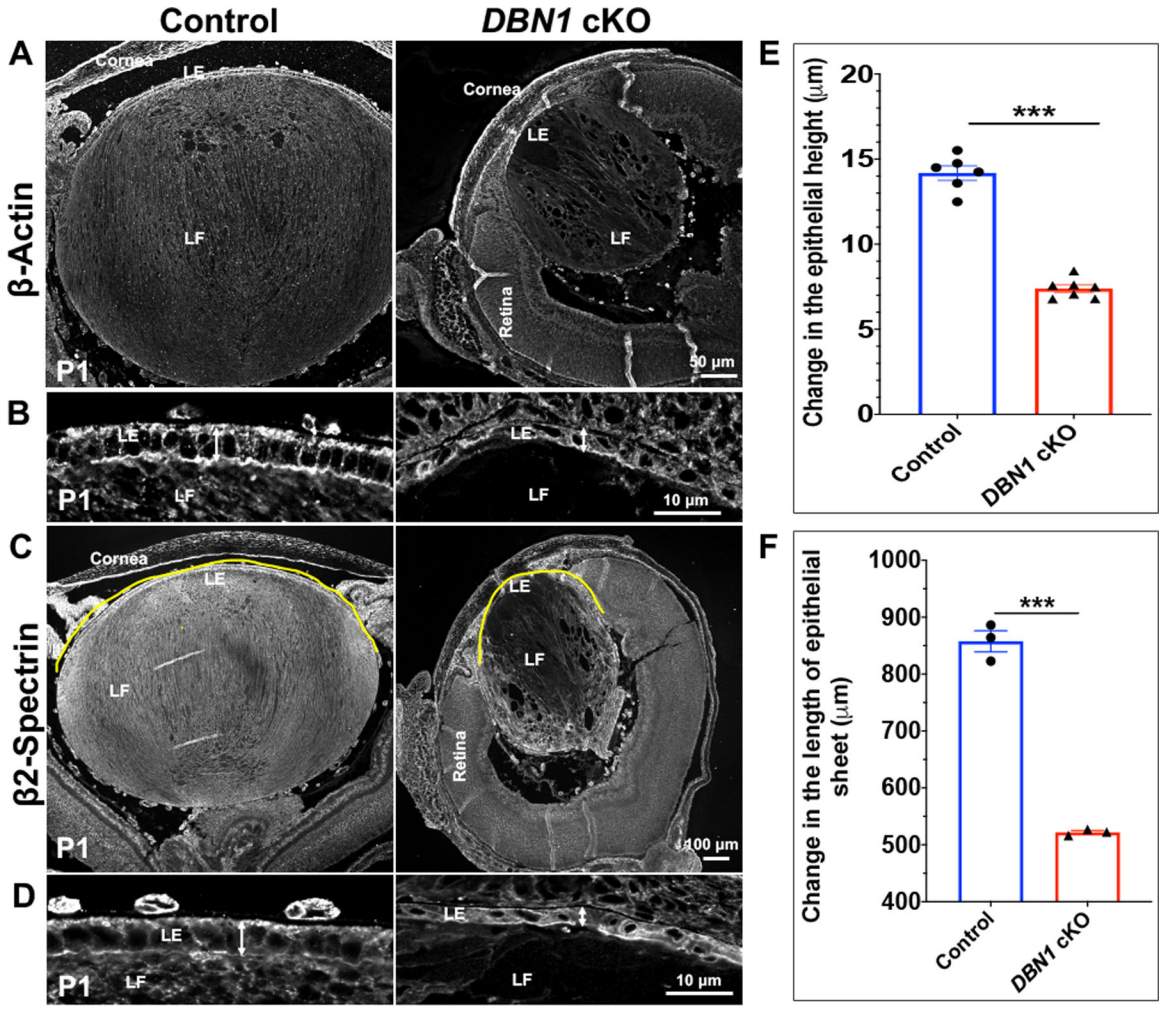

Figure 6: Drebrin deficiency impairs lens epithelial height, length, and disrupts spectrin-actin cytoskeletal organization in the mouse lens.

Sagittal sections of paraffin-embedded P1 eyes from *DBN1* cKO and littermate control mice were immunostained for β-actin (**A**) and β2-spectrin (**C**), and changes in lens epithelial height (double-headed arrows; **B, D, E**) and epithelial sheet width (yellow line; **C, F**) were evaluated. Both lens epithelial height and sheet width were significantly decreased (by ~50% and 40%, respectively) in drebrin cKO lenses compared to control lenses. Additionally, β-actin and β-spectrin immunostaining were also markedly decreased in lens fibers of drebrin cKO lenses compared to control lenses. The data in panels **E** and **F** present the mean±SEM values from 3–7 biological replicates. ***p < 0.001. LE: Lens epithelium, LF: Lens fibers. Scale bars; Image magnification.

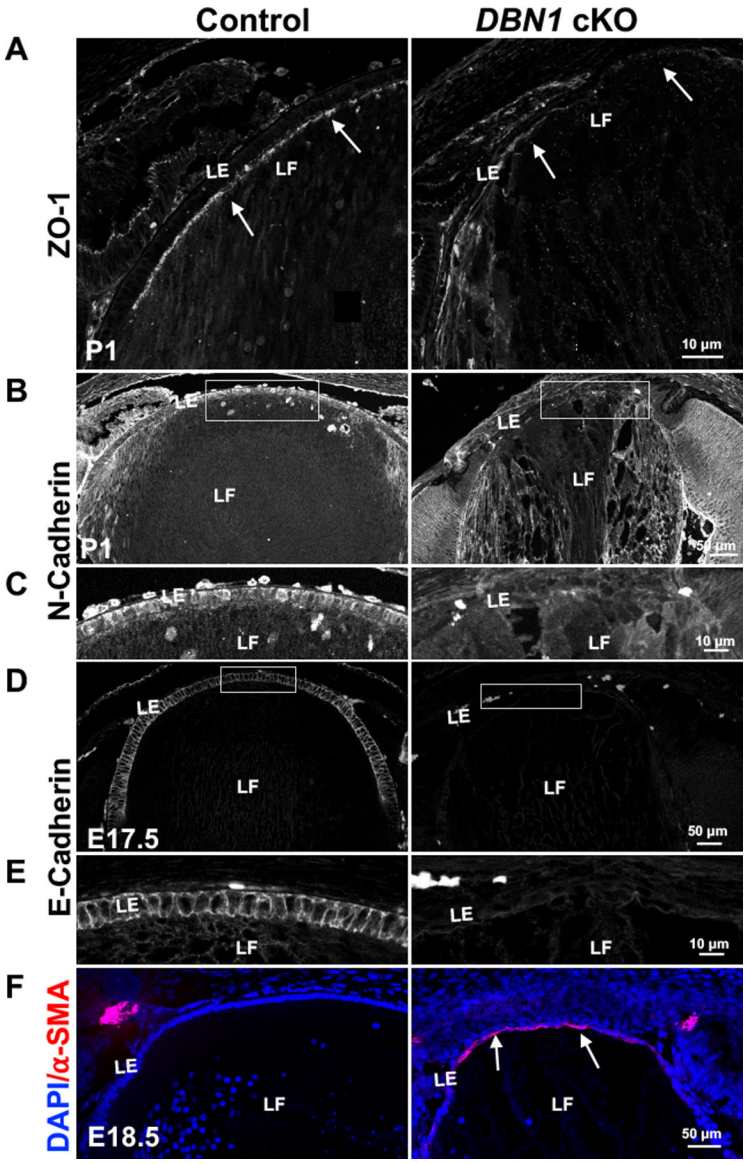

Figure 7: Drebrin deficiency disrupts cell-cell junctions and induces epithelial to mesenchymal transition in the mouse lens.

A) P1 drebrin cKO lenses reveal disruption in ZO-1 organization (immunofluorescence; arrows) relative to that noted for control lenses. Immunostaining of N-cadherin (**B and C**) in P1 and E-cadherin (**D and E**) in E17.5 drebrin cKO lenses reveals significantly reduced N-cadherin staining in both epithelium and fibers, and undetectable E-cadherin staining in the lens epithelium compared to control lenses. On the other hand, drebrin cKO lenses (E18.5) exhibit expression of α-SMA (immunofluorescence, arrows) in the epithelium (F), a marker of epithelial to mesenchymal transition, with α-SMA being undetectable in control lenses. These specimens were also co-stained for nuclei with DAPI (blue stain). LE: Lens epithelium; LF: Lens fiber cells. Scale bar; Image magnification.

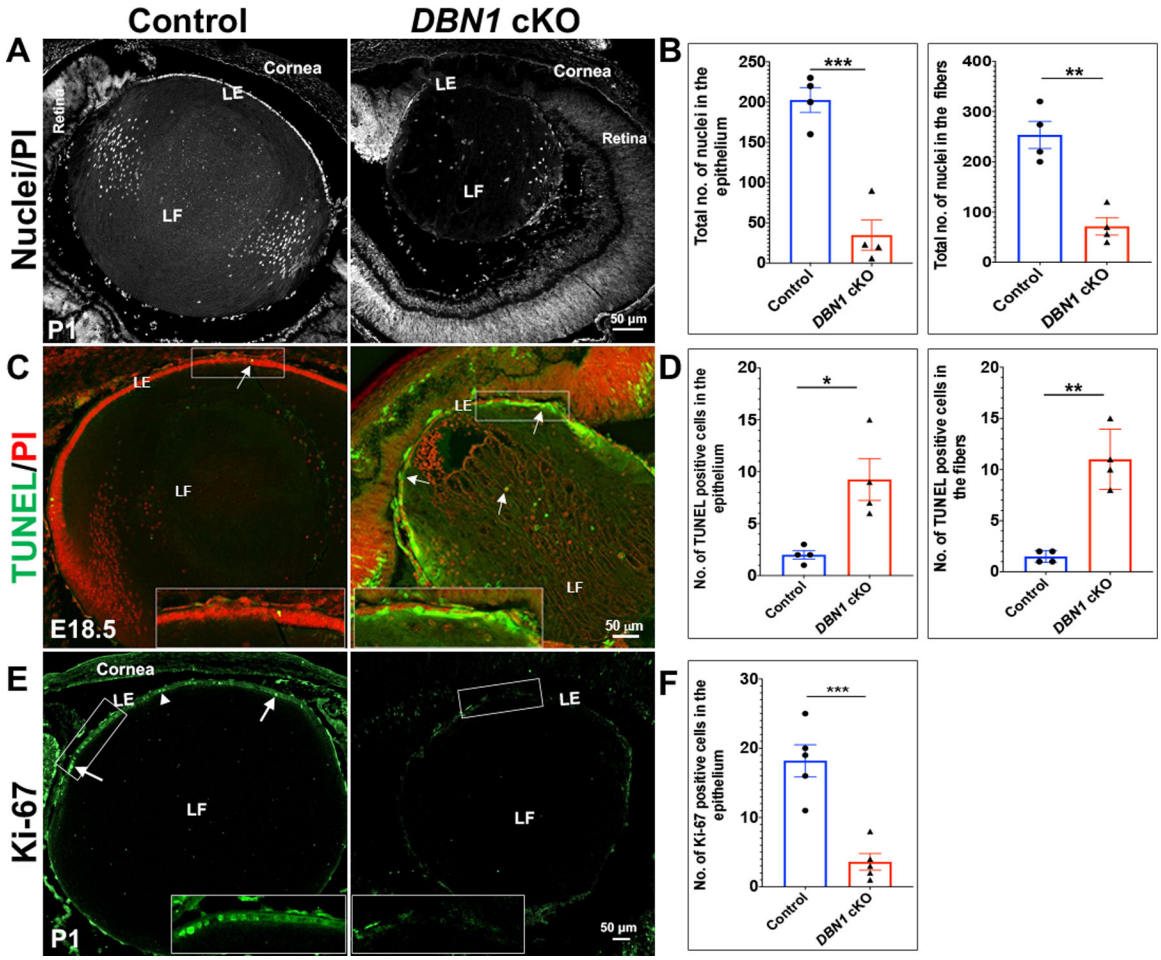

Figure 8: Impaired lens epithelial proliferation and survival in drebrin cKO lens.

A) Representative images of propidium iodide (PI) staining in control and drebrin cKO mouse lenses. **B)** Bar graphs showing a significant decrease in the number of total nuclei in the lens epithelium (by ~80%) and fibers (by ~70%) in drebrin cKO mice, compared to corresponding controls. **C)** Representative images of TUNEL staining (green fluorescence, arrows) in drebrin cKO and control mouse lenses with a magnified area of epithelium (insert). **D)** Quantitation of TUNEL positive cells in the lens epithelium and fiber cells of drebrin cKO mice showed a significant increase (by ~350% and 600% increase, respectively) in apoptotic cells (arrows) compared to control lenses. These specimens were also co-stained with propidium iodide (PI) to label cell nuclei. **E)** Representative immunofluorescence images of Ki-67 staining (green, arrows) in drebrin cKO and control mouse lenses. Inserts show a magnified area of epithelium. **F)** Quantitation of Ki-67 positive nuclei revealed a significant decrease (by ~ 80%) in proliferating cells in the epithelium of drebrin cKO lens compared to controls. Values are mean±SEM of ≥ 4 biological replicates. *P<0.05, **P<0.01 and ***P<0.001. LE: Lens epithelium; LF: Lens fiber cells. Scale bars; Image magnification.

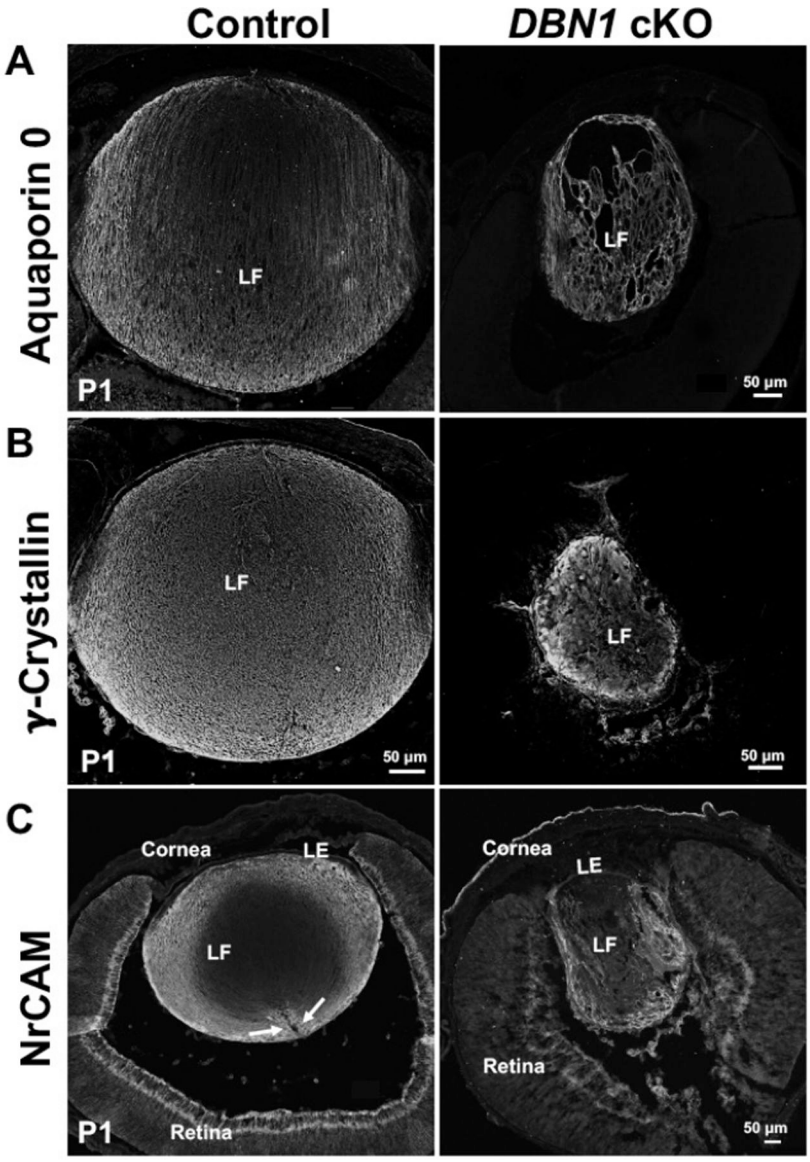

Figure 9: Impairment of fiber cell organization in drebrin deficient mouse lens.

To determine the possible involvement of drebrin in lens differentiation, P1 drebrin cKO, and control mouse lens specimens were immunostained for the fiber cell differentiation-specific markers AQP0, γ- crystalline and NrCAM. **A, B and C)** While the generation of differentiated fiber cells and positive immunostaining for AQP0, γ- crystallin and NrCAM are observed in drebrin cKO lenses, although not as robust as seen in the control lenses, indicating that drebrin deficiency does not, per se, affect the initiation of fiber cell differentiation. However, fiber cells are quite abnormal in length and organization in drebrin deficient lenses compared to control lenses. Arrows indicate suture formation in control lenses. LE: Lens epithelium; LF: Lens fiber cells. Scale bars; Image magnification.

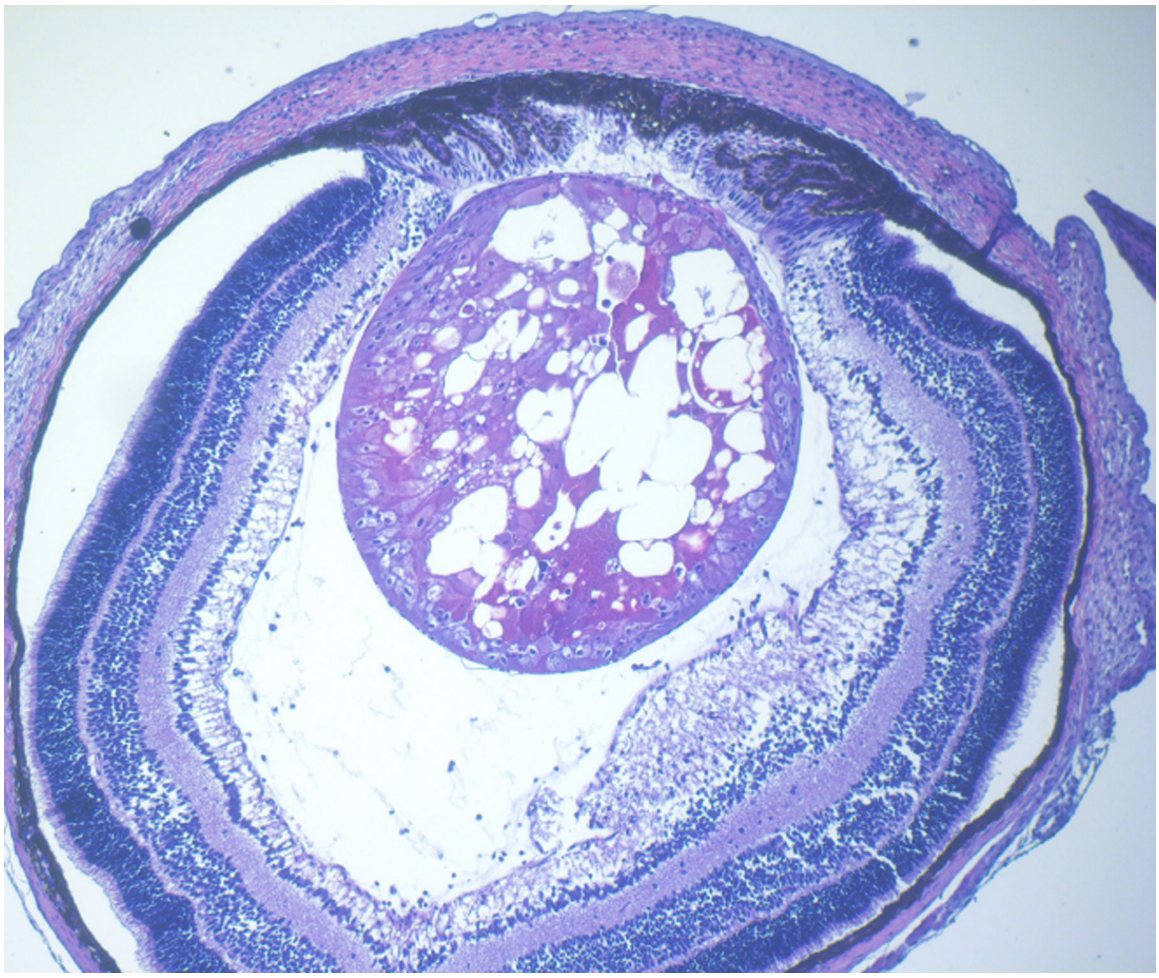

Fig. 10: Cover image:
Image of ocular lens defects in the neonatal drebrin conditional deficient mouse.

Table 1.

Antibodies used in immunostaining analysis

Antibodies	Cat. No.	Source	Dilution	Sections
Drebrin (Mouse Monoclonal)	BM5537	Origene Technologies Inc, Rockville, MD.	1:100	Paraffin
Drebrin (Rabbit Polyclonal)	ab60933	Abcam, Cambridge, UK	1:200	Cryo & Paraffin
β-Actin (Mouse Monoclonal)	8H10D10	Cell Signaling Technologies, Inc. Danvers, MA.	1:200	Paraffin
β2-Spectrin (Mouse Monoclonal)	612563	BD Biosciences, San Jose, CA.	1:200	Paraffin
E-Cadherin (Rabbit Polyclonal)	3195S	Cell Signaling Technology, Inc. Danvers, MA.	1:200	Paraffin
N-cadherin (Mouse Monoclonal)	33–3900	Life Technologies Corporation, Grand Island, NY	1:200	Paraffin
ZO-1 (Rabbit Polyclonal)	13663	Cell Signaling Technologies, Inc., Danvers, MA	1:200	Cryo
α-smooth muscle actin- Cy3 conjugated	C6198	Sigma-Aldrich, St. Louis, MO	1:200	Cryo
Ki-67 (Rabbit Polyclonal)	9129	Cell Signaling Technologies, Inc, Danvers, MA	1:200	Cryo
NrCAM (Rabbit Polyclonal)	ab24344–200	Abcam, Cambridge, UK	1:500	Paraffin
γ-Crystallin (Rabbit Polyclonal)		The Sam Zigler Laboratory, Johns Hopkins University School of Medicine. Baltimore, MD	1:500	Cryo
Aquaporin-0 (Rabbit Polyclonal)		The Joe Horwitz laboratory, Jules Stain Eye Institute, UCLA. CA	1:500	Cryo
Phalloidin–Tetramethylrhodamine B isothiocyanate (TRITC)	P1951	Sigma-Aldrich, St. Louis, MO	1:500	Cryo